Polymer Chemistry

PAPER

View Article Online
View Journal | View Issue

CrossMark click for updates

Cite this: *Polym. Chem.*, 2015, **6**, 4096

Cyclic polymers based on UV-induced strain promoted azide–alkyne cycloaddition reaction†

Peng Sun,[a] Qingquan Tang,[a] Zhenpeng Wang,[b] Yuming Zhao[a] and Ke Zhang*[a]

Received 21st March 2015,
Accepted 21st April 2015

DOI: 10.1039/c5py00416k

www.rsc.org/polymers

A unique method was developed for the preparation of cyclic polymers based on the combination of atom transfer radical polymerization (ATRP) and UV-induced strain promoted azide–alkyne cycloaddition (SPAAC) reaction. By virtue of a cyclopropenone-masked dibenzocyclooctyne functionalized ATRP initiator (**I-1**), well-defined telechelic polystyrene (PS) was synthesized to have a cyclopropenone-masked dibenzocyclooctyne at one polymer chain end and a bromo group at the other. The single electron transfer-nitroxide radical coupling reaction was then used to modify the bromo end group to azide, resulting in the corresponding linear PS precursor. Under UV irradiation on its highly diluted solution, the dibenzocyclooctyne end group was quantitatively released from cyclopropenone-masked dibenzocyclooctyne, which intramolecularly reacted with the azide end group *in situ* to ring-close the linear PS precursor and produce the corresponding cyclic PS based on the SPAAC click reaction.

Published on 22 April 2015. Downloaded by Michigan State University on 15/01/2016 12:54:32.

Introduction

Cyclic polymers have a fascinating macromolecular topology, in which the long polymer chain contains so many repeat units but no chain ends. This endows them with a series of physical properties which are significantly different from those of their linear polymer counterparts, including a smaller hydrodynamic volume and radius of gyration, lower melt viscosity, higher thermostability, and increased rate of crystallization.[1–7]

Thanks to the distinguished developments of living/controlled polymerization (CP) methods and click chemistry in polymer research fields, the combination of CP and click chemistry has been demonstrated as one of the most powerful methods for the formation of cyclic polymers. To date, a variety of combinations between CP and efficient coupling reactions have been developed to produce cyclic polymers, including atom transfer radical polymerization (ATRP)/copper-catalyzed azide–alkyne cycloaddition reaction (CuAAC),[8–13] ATRP/atom transfer radical coupling,[14,15] ATRP/ring-closing metathesis coupling,[16,17] ATRP/Diels–Alder reaction,[18,19] reversible addition–fragmentation chain transfer polymerization (RAFT)/CuAAC,[20,21] RAFT/thiol–ene reaction,[22,23] RAFT/thio–bromo reaction,[24] RAFT/Diels–Alder reaction,[25] ring-opening polymerization (ROP)/Diels–Alder reaction,[26] ROP/CuAAC,[27] and ROP/thiol–ene reaction.[28]

Among these combinations, the ATRP/CuAAC may be the most popular method used in the community, which was first introduced by Grayson's group.[8] In this technique, well-defined telechelic polymers were prepared by ATRP to have alkyne and bromo end groups. In the presence of NaN_3, the bromo end group was substituted by an azide to produce linear polymer precursors with the alkyne and azide separated at the polymer chain ends. In a highly diluted polymer solution, the CuAAC was performed intramolecularly to ring-close the linear precursors and produce the corresponding cyclic polymers. To date, this technique has been employed to prepare not only a variety of cyclic polymers including polystyrenics,[8,12,13] polyacrylamides,[9,10] and poly(methacrylates),[11] but also a library of cyclic topologies,[29–34] such as eight and tadpole shapes. The main disadvantage of the ATRP/CuAAC method, however, is the requirement of a large amount of copper catalyst to stimulate the CuAAC reaction for the ring-closure of linear precursors. This caused a big problem for purifying the resulting cyclic polymers, especially when the ring-closure strategies usually produce the cyclic polymer with a very low yield.

To overcome this, the strain promoted azide–alkyne cycloaddition (SPAAC) reaction has been developed and is widely used in the biological fields as a bioorthogonal reaction.[35,36] It has been demonstrated that the SPAAC shared the same reaction efficiency with CuAAC but eliminated the requirement of the copper catalyst.[35,36] Recently, we have successfully introduced the SPAAC reaction in the fields of topological polymer

[a]*State Key Laboratory of Polymer Physics and Chemistry, Institute of Chemistry, The Chinese Academy of Sciences, Beijing 100190, China.*
E-mail: kzhang@iccas.ac.cn; Fax: +86-010-62559373
[b]*National Center for Mass Spectrometry in Beijing, Institute of Chemistry, The Chinese Academy of Sciences, Beijing 100190, China*

†Electronic supplementary information (ESI) available: Experimental section and Fig. S1 and S2. See DOI: 10.1039/c5py00416k

This journal is © The Royal Society of Chemistry 2015

Published on 22 April 2015. Downloaded by Michigan State University on 15/01/2016 12:54:32.

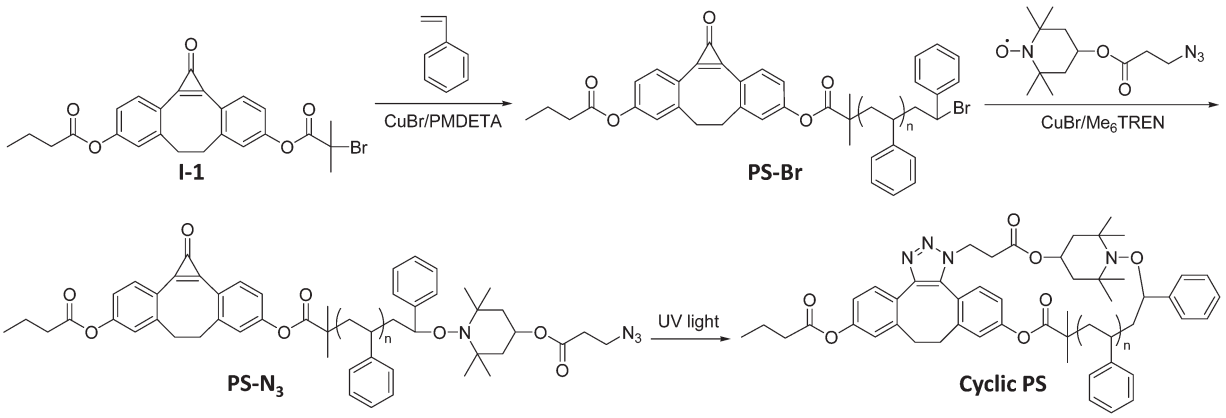

Scheme 1 Preparation of cyclic PS.

preparation.[37,38] Furthermore, by designing functional ATRP initiators having the cyclopropenone-masked dibenzocyclooctyne group, we successfully prepared well-defined polymethacrylates, polystyrenics, and polyacrylates functionalized with the cyclopropenone-masked dibenzocyclooctyne group from the standard ATRP technique.[39] The cyclopropenone-masked dibenzocyclooctyne has been demonstrated not to react with the azide group. Under UV irradiation, however, it could quantitatively release the reactive dibenzocyclooctyne group and SPAAC reaction could be performed *in situ* in the presence of an azide.[40,41] The UV-induced SPAAC technique is unique, because it not only allows one to control the reaction temporally and spatially, but also provides a practical way to introduce the dibenzocyclooctyne and azide groups in the same macromolecules. This largely extended the application of SPAAC reaction in fabricating the polymer topology such as cyclic polymers.

As a continuous contribution in this research topic herein, the combination of ATRP and UV-induced SPAAC click reaction was illustrated to construct the cyclic polymer topology. Scheme 1 shows the synthetic approach, in which the formation of cyclic PS was used as the model system to demonstrate the concept. From the functional ATRP initiator **I-1**, the well-defined telechelic PS (PS-Br) was prepared bearing cyclopropenone-masked dibenzocyclooctyne and bromo end groups. By virtue of the single electron transfer-nitroxide radical coupling (SET-NRC) reaction, the bromo group was efficiently changed to an azide, resulting in the linear PS precursor (PS-N_3) having cyclopropenone-masked dibenzocyclooctyne and azide end groups. Under UV irradiation and in a highly diluted solution, the UV-induced SPAAC click reaction was carried out intramolecularly to ring-close the linear PS-N_3 precursor and produce the corresponding cyclic PS.

Experimental

Experimental details are given in the ESI.†

Results and discussion

Using initiator **I-1**, the ATRP of styrene was performed in bulk at 90 °C with $[St]_0/[\mathbf{I\text{-}1}]_0/[PMDETA]_0/[CuBr]_0$ = 100/1/1/1 to produce the PS-Br (the first step in Scheme 1). A monomer conversion of *ca*. 18% was obtained in 25 min by this polymerization condition. Fig. S1† shows the GPC curve (black) of the resulting PS-Br, in which a monomodal and symmetric peak was obtained corresponding to the M_n and PDI (M_w/M_n) of 2370 and 1.06. Fig. 1B shows the corresponding ^{1}H-NMR spectrum, where the characteristic proton signals of Ha, Hd, Hd′, and Hf were preserved in the resulting PS-Br from the initiator **I-1** (Fig. 1A). In addition, the area ratio of 1/2 between peaks Hl and Ha indicated that the cyclopropenone-masked dibenzocyclooctyne group was introduced in each polymer chain and the preparation of telechelic PS-Br was successful.

The azide group was subsequently introduced at the end of PS by replacing the bromo end group by virtue of the SET-NRC technique (the second step in Scheme 1). To achieve a quantitative reaction efficiency, the molar ratio of 1.5 was used between 4-(3-azidopropionyloxy)-2,2,6,6-tetramethylpiperidine-1-oxyl (TEMPO-N_3) and PS-Br. The SET-NRC was performed in the mixed solvents of toluene and DMSO (v/v = 1/1) at room temperature for 20 min in the presence of CuBr and Me_6TREN. Fig. S1† (red) shows the GPC curve of the resulting PS-N_3, in which a monomodal and symmetric peak shape was preserved and the peak position shifted to the higher molecular weight direction completely, compared to that of the PS-Br precursor (black curve). The M_n and PDI were integrated as 2760 and 1.06, respectively. Fig. S2† (red curve) shows the corresponding FT-IR adsorption spectrum, where the characteristic azide adsorption peak was observed at 2100 cm^{-1}, compared to that of the PS-Br precursor (black curve). Fig. 1C shows the ^{1}H-NMR spectrum of the resulting PS-N_3, in which the new proton signals of Hm and Hn appeared at 4.95 and 3.53 ppm, ascribed to the newly introduced TEMPO-N_3 end group. In addition, the area ratio of 2/1/2 among Ha/Hm/Hn indicated a quantitative reaction efficiency. Fig. 2A (red curve) shows the corresponding UV-VIS adsorption spectrum, in which a typical

Published on 22 April 2015. Downloaded by Michigan State University on 15/01/2016 12:54:32.

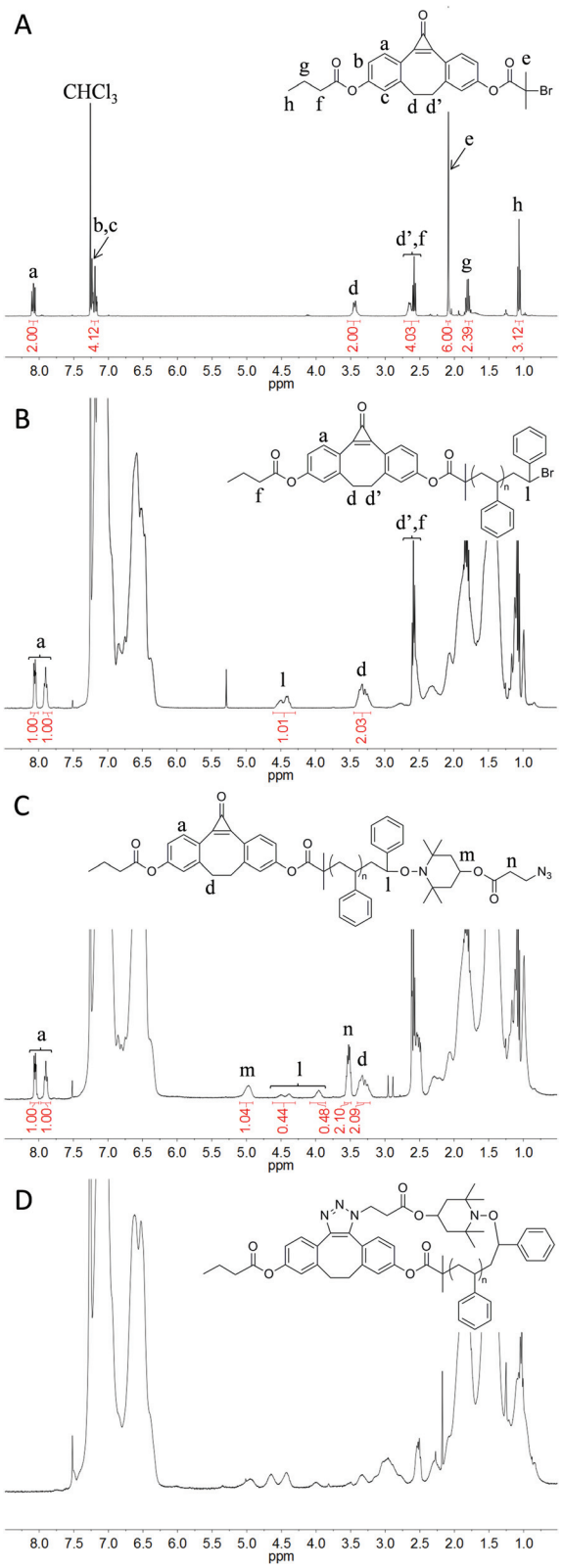

Fig. 1 ^{1}H-NMR spectra of functional ATRP initiator **I-1** (A) and the resulting PS-Br (B), PS-N_3 (C), and cyclic PS (D). $CDCl_3$ was used as a deuterated solvent.

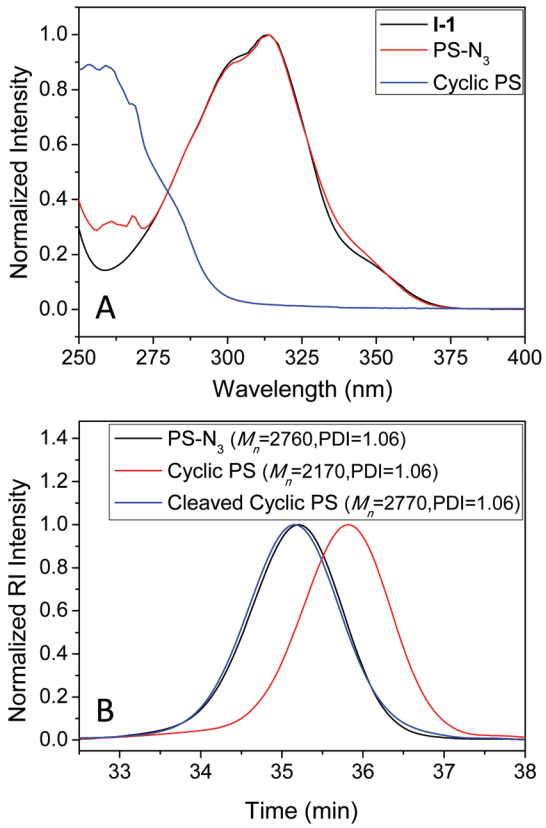

Fig. 2 (A) UV-VIS adsorption spectra of functional ATRP initiator **I-1** (black) and the resulting PS-N_3 (red) and cyclic PS (blue), in which THF was used as the solvent for measurements. (B) GPC data of PS-N_3 (black), cyclic PS (red), and the thermally cleaved cyclic PS (blue), in which THF was used as the eluent and PS standards were used for the calibration.

strong adsorption band was observed with a peak position at 314 nm ascribed to the cyclopropenone-masked dibenzocyclooctyne group. In addition, the spectrum was completely overlapped with that (black curve) of the initiator **I-1**, indicating that the cyclopropenone-masked dibenzocyclooctyne group survived from the used ATRP and SET-NRC reaction conditions.

After successful preparation of PS-N_3, the UV-induced SPAAC was employed to ring-close the linear precursor and produce the cyclic PS (the third step in Scheme 1). The regular low pressure mercury lamp (120 W) was used as a UV light source to deprotect the cyclopropenone-masked dibenzocyclooctyne group. After applying 5 h UV irradiation on a PS-N_3 diluted solution (7 mg/30 mL, 1×10^{-4} mol L^{-1}) in the mixed solvents of THF/MeOH (v/v = 1/2), the reaction mixture was kept stirring for another 36 h to produce the well-defined cyclic PS.

The characterization was performed by a combination of UV-VIS, ^{1}H-NMR, FT-IR, GPC, and MALDI-TOF MS to demonstrate the successful UV-induced SPAAC reaction and the formation of cyclic polymers. From the UV-VIS adsorption spectra (Fig. 2A), the adsorption peak of the cyclopropenone-masked

 This journal is © The Royal Society of Chemistry 2015

Published on 22 April 2015. Downloaded by Michigan State University on 15/01/2016 12:54:32.

dibenzocyclooctyne group at 314 nm completely disappeared from the curve of the resulting cyclic PS (blue), compared to that (red curve) of the linear PS-N_3 precursor. In addition, from the ^{1}H-NMR spectrum (Fig. 1D), the characteristic Ha proton signals of the cyclopropenone-masked dibenzocyclooctyne group completely disappeared at 8.06 and 7.90 ppm after the formation of cyclic PS, compared to that of the linear PS-N_3 precursor (Fig. 1C). Fig. S2† (blue) shows the corresponding FT-IR curve, where the azide adsorption peak completely disappeared at 2100 cm^{-1}, compared to that (red curve) of the linear PS-N_3 precursor. These strongly indicated that a high reaction efficiency was achieved for the UV-induced SPAAC reaction under the used conditions.

The formation of cyclic PS topology was verified by GPC and MALDI-TOF MS analyses. As shown in Fig. 2B, the GPC curve (red) of the resulting cyclic PS preserved the well-defined monomodal and symmetric peak shape but the whole peak position shifted to the lower molecular weight direction completely, compared to that (black curve) of the linear precursor. The integration of GPC curves produced the same PDI of 1.06 and a 0.79 times smaller M_n (2170 for cyclic PS *vs.* 2760 for linear PS) between cyclic and linear PS. Fig. 3 shows the MALDI-TOF MS of linear (A) and cyclic PS (B). As shown in the full spectra (left), the absolute molecular weights were similar for both cases expanding from 2000 to 3600. Compared to the apparent M_n ratio of 0.79 between the cyclic PS and the linear precursor from GPC characterization, a similar absolute molecular weight indicated a more compact molecular structure for cyclic PS, strongly indicating the successful formation of cyclic topology. From the expanded spectra (right), the main peak distribution of the linear PS could be accurately assigned to linear PS with an elimination of N_2 ionized with H^+.[8,42,43] For the cyclic PS, the main peak distribution was precisely ascribed to the cyclic PS ionized with H^+. A regular *m*/*z* interval of *ca.* 104 was observed between neighboring peaks in the main distribution for both cases, which corresponds to the molar mass of the St monomer unit. In this specific case, the linear and cyclic PS shared the similar peak values measured from MALDI-TOF MS in a linear mode (Fig. 3). To confirm our peak assignments for linear PS with the loss of N_2 but not CO (Fig. 3A), matrix-assisted laser desorption/ionization Fourier transform ion cyclotron resonance mass spectrometry was used for further characterization. Due to the very high resolution, this technique could accurately detect the slight *m*/*z* difference of the linear PS-N_3 species between losing N_2 and CO. As shown in Fig. S3,† for peak a (the same signal of a in Fig. 3A) of linear PS_{19} with an elimination of N_2 ionized with H^+, the measured *m*/*z* of 2622.50655 correlated well with that (2622.50645) of the theoretical value. For the corresponding cyclic PS_{19} from linear PS_{19} with losing CO ionized by H^+ (Fig. S4,† peak a, the same signal of a in Fig. 3B), however, the measured *m*/*z* was 2622.51744 in good agreement with that (2622.51768) of the theoretical one.

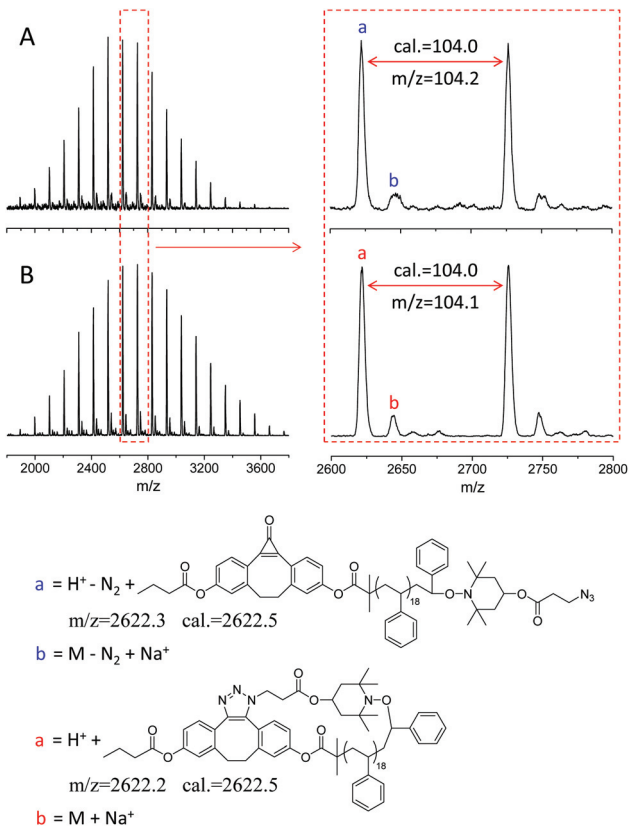

Fig. 3 MALDI-TOF MS of the linear PS-N_3 precursor (A) and the resulting cyclic PS (B).

The novel ring-closure method produced the cyclic polymer chain with a heat-liable NO–C bond at the nitroxide linkage, which allowed cyclic polymers to be cleaved by a convenient thermolysis process. After heating the cyclic PS at 150 °C for 48 h under N_2, the resulting linear PS was characterized by GPC. As shown in Fig. 2B, compared to that (red curve) of cyclic PS, the GPC curve (blue) of the thermally cleaved cyclic PS shifted completely to a higher molecular weight direction and nearly overlapped with that of the linear PS-N_3 precursor (black curve). The corresponding M_n and PDI were calculated as 2770 and 1.06, respectively. The successful return to the original apparent molecular weight of the linear PS-N_3 precursor (M_n = 2760) upon ring-opening by thermolysis again strongly confirmed the formation of the cyclic PS topology.

Finally, a batchwise operation was combined with this novel ring-closure technique to improve the notorious low yield disadvantage of the ring closure strategy for cyclic polymers. As an example, a 3 times more linear PS-N_3 (21 mg) was evenly added into 30 mL solvents in 3 batches by alternating every 5 h UV irradiation, by which the starting polymer concentration was kept the same as that of the regular one batch operation (7 mg/30 mL). After the addition, the cyclization reaction was allowed to perform for 24 h more. Fig. S5† shows the GPC curve (red) of the resulting cyclic PS, which completely overlapped with that (black curve) of cyclic PS from the regular one batch operation. Resultantly, this method could conveniently produce pure cyclic polymers with increased yield by virtue of the batchwise operation.

Published on 22 April 2015. Downloaded by Michigan State University on 15/01/2016 12:54:32.

Conclusions

In conclusion, we developed a novel, simple, clean, and efficient ring-closure method for the formation of cyclic polymers by combining ATRP and UV-induced SPAAC click reaction. The distinct advantages of this technique include the following two aspects. First, the ring-closure of linear polymer precursors was performed in air at room temperature without any other catalyst or stimulus requirements other than mild UV irradiation. As a result, the formed pure cyclic polymers could be conveniently collected only by evaporating the solvents. Second, a heat-liable NO–C bond was designed in the cyclic polymer chain at the nitroxide linkage, which facilitated the cyclic polymers to be cleaved back to its linear counterparts by a convenient thermolysis when necessary. Inspired by the successful preparation of cyclic PS, the following research studies are being carried out in our group mainly focusing on three directions. One is expanding this technique to prepare more types of cyclic polymers including polyacrylates and poly (methacrylates). The other is to prepare various cyclic polymer derivatives with advanced topologies such as tadpole, eight, and flower-like shapes by virtue of the multi-functional ATRP initiators based on the same combination technique. The last one is to develop the catalyst-free ring-closure method for preparing cyclic polyester biomaterials from the combination between ROP and UV-induced SPAAC reaction.

Acknowledgements

Generous support was primarily provided by the Ministry of Science and Technology of China (2014CB932200 and 2012CB933200) and the National Science Foundation of China (21374122). K. Z. thanks the *Bairen* project from The Chinese Academy of Sciences for support.

Notes and references

1 K. Zhang and G. N. Tew, *React. Funct. Polym.*, 2014, **80**, 40.
2 Z. F. Jia and M. J. Monteiro, *J. Polym. Sci., Part A: Polym. Chem.*, 2012, **50**, 2085.
3 T. Yamamoto and Y. Tezuka, *Polym. Chem.*, 2011, **2**, 1930.
4 J. N. Hoskins and S. M. Grayson, *Polym. Chem.*, 2011, **2**, 289.
5 H. R. Kricheldorf, *J. Polym. Sci., Part A: Polym. Chem.*, 2010, **48**, 251.
6 B. A. Laurent and S. M. Grayson, *Chem. Soc. Rev.*, 2009, **38**, 2202.
7 K. Endo, *Adv. Polym. Sci.*, 2008, **217**, 121.
8 B. A. Laurent and S. M. Grayson, *J. Am. Chem. Soc.*, 2006, **128**, 4238.
9 J. Xu, J. Ye and S. Liu, *Macromolecules*, 2007, **40**, 9103.
10 X. P. Qiu, F. Tanaka and F. M. Winnik, *Macromolecules*, 2007, **40**, 7069.
11 Z. Ge, Y. Zhou, J. Xu, H. Liu, D. Chen and S. Liu, *J. Am. Chem. Soc.*, 2009, **131**, 1628.
12 D. E. Lonsdale, C. A. Bell and M. J. Monteiro, *Macromolecules*, 2010, **43**, 3331.
13 X. Zhu, N. Zhou, Z. Zhang, B. Sun, Y. Yang, J. Zhu and X. Zhu, *Angew. Chem., Int. Ed.*, 2011, **50**, 6615.
14 A. F. Voter, E. S. Tillman, P. M. Findeis and S. C. Radzinski, *ACS Macro Lett.*, 2012, **1**, 1066.
15 S. S. Wang, K. Zhang, Y. M. Chen and F. Xi, *Macromolecules*, 2014, **47**, 1993.
16 K. Adachi, S. Honda, S. Hayashi and Y. Tezuka, *Macromolecules*, 2008, **41**, 7898.
17 E. Baba, S. Honda, T. Yamamoto and Y. Tezuka, *Polym. Chem.*, 2012, **3**, 1903.
18 H. Durmaz, A. Dag, G. Hizal and U. Tunca, *J. Polym. Sci., Part A: Polym. Chem.*, 2010, **48**, 5083.
19 M. Glassner, J. P. Blinco and C. Barner-Kowollik, *Macromol. Rapid Commun.*, 2011, **32**, 724.
20 A. S. Goldmann, D. Quémener, P. Millard, T. Davis, M. Stenzel, C. Barner-Kowollik and H. E. Müller, *Polymer*, 2008, **49**, 2274–2281.
21 M. D. Hossain, D. Valade, Z. Jia and M. J. Monteiro, *Polym. Chem.*, 2012, **3**, 2986–2995.
22 D. Lu, Z. Jia and M. J. Monteiro, *Polym. Chem.*, 2013, **4**, 2080.
23 B. Liu, H. Wang, L. Zhang, G. Yang, X. Liu and I. Kim, *Polym. Chem.*, 2013, **4**, 2428.
24 S. Y. Long, Q. Q. Tang, Y. Wu, L. X. Wang, K. Zhang and Y. M. Chen, *React. Funct. Polym.*, 2014, **80**, 15.
25 Q. Q. Tang, Y. Wu, P. Sun, Y. M. Chen and K. Zhang, *Macromolecules*, 2014, **47**, 3775.
26 T. Josse, O. Altintas, K. K. Oehlenschlaeger, P. Dubois, P. Gerbaux, O. Coulembier and C. Barner-Kowollik, *Chem. Commun.*, 2014, **50**, 2024.
27 J. N. Hoskins and S. M. Grayson, *Macromolecules*, 2009, **42**, 6406.
28 M. J. Stanford, R. L. Pflughaupt and A. P. Dove, *Macromolecules*, 2010, **43**, 6538.
29 D. E. Lonsdale and M. J. Monteiro, *Chem. Commun.*, 2010, **46**, 7945.
30 B. V. K. J. Schmidt, N. Fechler, J. Falkenhagen and J. F. Lutz, *Nat. Chem.*, 2011, **3**, 234.
31 X. Fan, B. Huang, G. Wang and J. Huang, *Macromolecules*, 2012, **45**, 3779.
32 Z. Jia, D. E. Lonsdale, J. Kulis and M. J. Monteiro, *ACS Macro Lett.*, 2012, **1**, 780.
33 J. Jeong, K. Kim, R. Lee, S. Lee, H. Kim, H. Jung, M. A. Kadir, Y. Jang, H. B. Jeon, K. Matyjaszewski, T. Chang and H. J. Paik, *Macromolecules*, 2014, **47**, 3791.
34 M. D. Hossain, Z. Jia and M. J. Monteiro, *Macromolecules*, 2014, **47**, 4955.
35 E. M. Sletten and C. R. Bertozzi, *Acc. Chem. Res.*, 2011, **44**, 666.
36 M. F. Debets, S. S. Van Berkel, J. Dommerholt, A. J. Dirks, F. P. Rutjes and F. L. Van Delft, *Acc. Chem. Res.*, 2011, **44**, 805.

 This journal is © The Royal Society of Chemistry 2015

37 X. K. Yang, S. S. Wang, Y. C. Yan, Y. Wu, K. Zhang and Y. M. Chen, *Polymer*, 2011, **55**, 1128.
38 S. S. Wang, X. K. Yang, W. Zhu, L. Zou, K. Zhang, Y. M. Chen and F. Xi, *Polymer*, 2011, **55**, 4812.
39 P. Sun, G. W. Yan, Q. Q. Tang, Y. M. Chen and K. Zhang, *Polymer*, 2015, **64**, 202.
40 A. A. Poloukhtine, N. E. Mbua, M. A. Wolfert, G. J. Boons and V. V. Popik, *J. Am. Chem. Soc.*, 2009, **131**, 15769.
41 S. V. Orski, A. A. Poloukhtine, S. Arumugam, L. Mao, V. V. Popik and J. Lcoklin, *J. Am. Chem. Soc.*, 2010, **132**, 11024.
42 Y. Li, J. N. Hoskins, S. G. Sreerama and S. M. Grayson, *Macromolecules*, 2010, **43**, 6225.
43 T. Josse, J. De Winter, P. Dubois, O. Coulembier, P. Gerbaux and A. Memboeuf, *Polym. Chem.*, 2015, **6**, 64.

Published on 22 April 2015. Downloaded by Michigan State University on 15/01/2016 12:54:32.